Structure Effects of Double D-Amino Acid Replacements: A Nuclear Magnetic Resonance and Circular Dichroism Study Using Amphipathic Model Helices†

Sven Rothemund,‡ Michael Beyermann,‡ Eberhard Krause,‡ Gerd Krause,‡ Michael Bienert,‡ Robert S. Hodges,§,|| Brian D. Sykes,§,|| and Frank D. Sönnichsen*,||

Institute of Molecular Pharmacology, Alfred-Kowalke-Strasse 4, 10315 Berlin, Germany, Department of Biochemistry and Medical Research Council of Canada Group in Protein Structure and Function, University of Alberta, Edmonton, Alberta T6G 2H7, Canada, and Protein Engineering Network of Centres of Excellence, Department of Biochemistry, University of Alberta, Heritage Medical Research Centre 7-13, Edmonton, Alberta T6E 2S2, Canada

Received April 17, 1995⊗

ABSTRACT: D-Amino acid replacements and the determination of resulting structural changes are a useful tool to recognize amphipathic helices in biologically active peptides such as neuropeptide Y and corticotropin-releasing factor. In this paper the secondary structures of one amphipathic α-helical peptide and its double D-amino acid analog have been determined by means of ^{1}H NMR and CD spectroscopies under equivalent conditions. The chemical shifts (NH and CαH) and the analysis of nuclear Overhauser effects show a split of the continuous helix for the all-L peptide into two helices at the position of double D-amino acid replacement. Hydrogen exchange rates correlate with water accessibilities in the hydrophobic/hydrophilic face and confirm the amphipathic helical structure in the all-L peptide as well as in its double D-amino acid analog. A significantly accelerated hydrogen isotope exchange rate is observed for the D-Ala^9 backbone proton, implying an increased flexibility at that position. These results show that the incorporation of an adjacent pair of D-amino acids only causes a local change in structure and flexibility, which makes the double D replacement interesting as a tool for specific helix-disturbing modifications to search for helical conformations in biologically active peptides.

Amphipathic helices are structural motifs often found in biologically active peptides and proteins (Segrest et al., 1990; Kaiser & Kezdy, 1983). The recognition and localization of helical structures at specific sites of a peptide or protein are important not only for the structural characterization of membrane-associating peptides but also for understanding the folding of polypeptide chains into their biologically active conformation (Scholz & Baldwin, 1992).

Sophisticated physical methods, such as X-ray crystallography or NMR[1] spectroscopy, allow the determination of secondary structures in the crystal or in solution, respectively. Equally, structural changes induced by specific local modifications of the primary sequence in combination with simple analytical methods can be used to provide information on the structure at the substituted site. In one such approach, single-point modifications at each amino acid along the peptide sequence and the determination of their structural influence for each analog yield information on the location of helical structure. This approach has the advantage that the substituted analogs can be applied at the same time to biological assays to investigate the biological importance of a helical structure motif.

An effective modification to disturb helical peptide structures is given by removing the proton at backbone amides, which can be achieved by replacing an amino acid by proline (Strehlow et al., 1991; Barlow et al., 1988; MacArthure et al., 1991) or by its corresponding N-methylated amino acid (Rivier et al., 1993). The replacement by proline might cause a drastic change of the side-chain functionality at the same time, making the interpretation of biological results difficult. The chemical incorporation of N-methylated amino acids requires special chemical conditions and often results in low product yields due to steric hindrance (Rivier et al., 1993). D-Amino acid replacement was also found to disturb helical structures (Fairman et al., 1992). Due to the advantage of retained side-chain functionality, D-amino acid scans were frequently used for the elucidation of the biological importance of helical structures in peptides (Beck-Sickinger et al., 1990; Chen et al., 1990; Pounny & Shai, 1992; Peeters et al., 1992).

Previous investigations of the structural influence of single D-amino acid replacements at each position along amphipathic model peptides have shown that a single replacement may not always be sufficient for a reliable determination of a structural effect (Fairman et al., 1992; Krause et al., 1995). Pairwise substitution of adjacent amino acids by their

† This work was supported by a grant from the Deutsche Forschungsgemeinschaft (Kr 1451/2-1).

* To whom correspondence should be addressed.

‡ Institute of Molecular Pharmacology.

§ Department of Biochemistry and Medical Research Council of Canada Group in Protein Structure and Function, University of Alberta.

|| Protein Engineering Network of Centres of Excellence, Department of Biochemistry, University of Alberta.

⊗ Abstract published in *Advance ACS Abstracts,* September 15, 1995.

[1] Abbreviations: ACN, acetonitrile; 1D, one dimensional; 2D, two dimensional; 3D, three dimensional; CRF, corticotropin-releasing factor; CD, circular dichroism; COSY, correlation spectroscopy; DIEA, diisopropylethylamine; DMF, dimethylformamide; DSS, 4,4-dimethyl-4-silapentane-1-sulfonate; HPLC, high-performance liquid chromatography; MD, molecular dynamics; NMR, nuclear magnetic resonance; NOE, nuclear Overhauser effect; NOESY, nuclear Overhauser enhancement spectroscopy; NPY, neuropeptide Y; SA, simulated annealing; TBPipU, 2-(1*H*-benzotriazol-1-yloxy)-1,1,3,3-bis(pentamethylene)uronium tetrafluoroborate; TFA, trifluoroacetic acid; TFE, 2,2,2-trifluoroethanol; TOCSY, total correlation spectroscopy.

0006-2960/95/0434-12954$09.00/0

corresponding D-amino acids provides a much more pronounced helix disturbance. Studying the chromatographic retention behavior of these double D-amino acid replacement analogs has been successfully applied to recognize amphipathic helices in NPY and CRF (Krause et al., 1995). It was shown that the replacements show a characteristic HPLC retention time pattern indicating the location of amphipathic α-helices. The effect is caused by the disturbance of the preferred hydrophobic binding domain of the stationary-phase-bound peptide. Subsequent studies have demonstrated that these "retention time profiles" can also be observed in less amphipathic peptides (Rothemund et al., 1995), although the effect is less pronounced. In the case of an amphipathic α-helix two adjacent D-amino acids incorporated in the center of the helix reduce the HPLC retention time significantly by 30%. These results raised the question of the detailed structural influence of double D-amino acid replacements on the helical conformation, in particular, whether the obtained retention time profiles are caused by specific disturbance of the helical structure in definite positions or by an overall helix destabilization.

Several CD studies of helix-breaking or helix-destabilizing substitutions have been reported (Altmann et al., 1990; O'Neil & DeGrado, 1990; Strehlow et al., 1991; Chakrabartty et al., 1991) but only a few NMR studies (Gurunath & Balaram, 1994). In order to study the effect of "DD" substitutions on the structure, we decided to apply CD spectroscopy and NMR spectroscopy to distinguish local from overall structural changes. We synthesized a de novo amphipathic α-helical model peptide and its double D-amino acid analog. As a representative analog we chose the peptide with DD replacement at positions 9 and 10, since this replacement has the strongest effect on helicity. We have examined the structures of both the model peptide and its DD analog by ^{1}H NMR spectroscopy in 50% TFE to mimic the conditions present during CD and, potentially, during interactions of peptides with biological membranes which become active by assuming a helical secondary structure (Nelson & Kallenbach, 1986; Sönnichsen et al., 1992; Jackson & Mantsch, 1992).

MATERIALS AND METHODS

Peptide Synthesis and Purification. The peptide Ac-KLLKLAAKALLKLLKLAA-NH_2 and its corresponding D-amino acid analog Ac-KLLKLAA**dal**LKLLKLAA-NH_2 were synthesized by the solid-phase method using Fmoc strategy on a MilliGen 9050 peptide synthesizer. The peptide with 18 L-amino acids is denoted as LA-18 (L-amino acids, amphipathic, 18 residues), and the peptide with the two D-amino acids, D-Ala and D-Leu at positions 9 and 10, is denoted as DA-18 (two D-amino acids, amphipathic, 18 residues). To promote the helical content and suppress unfavorable charge−helix dipole interactions, all peptides were N-terminally acetylated and C-terminally amidated (Shoemaker et al., 1987).

All amino acids were coupled using TBPipU (Henklein et al., 1991), and the Fmoc groups were removed at each cycle with 20% piperidine in DMF. The peptides were acetylated with 20% acetic anhydride/70% DMF/10% DIEA (v/v/v). The peptides were cleaved from the resin support (TentaGel S RAM resin, 0.2 mmol/g, Rapp Polymere, Tübingen) with 90% TFA/5% thioanisole/5% *m*-cresol (v/v/v) for 3 h at ambient temperature.

Purification of crude peptides was carried out by preparative reversed-phase chromatography on PolyEncap A300, 10 μm, 250 × 20 mm i.d. (Bischoff Analysentechnik GmbH, Leonberg). Mobile phase A was 0.1% TFA in water, B was 50% ACN/50% water (v/v), and the linear AB gradient was 1.3% B/min. The peptides gave correct values in amino acid analysis using a LC3000 amino acid analyzer (Biotronik, Eppendorf) and gave expected $[M + H]^+$ mass peaks by matrix-assisted laser desorption/ionization mass spectroscopy (Maldi II, Kratos, Manchester).

Size-exclusion chromatography (SEC) was carried out on a Spherogel TSK-2000SW column (300 × 7.5 mm i.d., Pharmacia LKB, Uppsala) at a flow rate of 1 mL/min at ambient temperature. The mobile phase was 50% TFE/50% 0.1 M KH_2PO_4, pH 2.5, 25 °C. A linear relationship between molecular weight and peptide retention time during SEC for three standard reference peptides and the two model peptides LA-18 and DA-18 was found, indicating that the peptides LA-18 and DA-18 are monomeric at high concentrations of 2.5 mM in 50% TFE (Lau et al., 1984).

^{1}H NMR Spectroscopy. The peptides were dissolved in 50% TFE-d_3/50% H_2O (v/v) at a final peptide concentration of 2.5 mM. The pH was adjusted to 2.5 with 0.1 M DCl. The ^{1}H NMR spectra were acquired at 25 °C on Varian Unity-300 and VXR-500 spectrometers. All spectra were referenced to the methyl resonance of DSS at 0.0 ppm, which was added as internal standard. The observed proton resonance line widths under these conditions were expected for structured peptides of this molecular weight, which indicated the absence of aggregation effects.

Typical acquisition parameters at 500 MHz were a spectral width of 6000 Hz and a pulse width (90°) of 8.7 μs. The suppression of the H_2O resonance was accomplished by a 2.0 s presaturation pulse. One-dimensional spectra were acquired using 256 transients and 20032 data points and were zero filled to 65 536 data points. For two-dimensional spectra 2048 complex data points, 32 transients, and 256 complex increments were acquired. Double-quantum-filtered phase-sensitive 2D correlated spectroscopy (DQF-COSY; Piantini et al., 1982; Rance et al., 1983) and 2D total correlation spectroscopy (TOCSY; Braunschweiler & Ernst, 1983; Davis & Bax, 1985) were used for spin-type assignment. Sequential assignments were made using phase-sensitive 2D nuclear Overhauser effect spectroscopy (NOESY; Jeener et al., 1979) and standard procedures (Wüthrich, 1986). Several mixing times between 100−200 ms for NOESY and 65−80 ms for TOCSY spectra were acquired. The 2D data were processed on a SUN-IPC workstation using the Varian software (VNMR 4.3A).

Hydrogen exchange rates were determined at 25 °C with a 2.5 mM peptide solution freshly dissolved in 50% TFE-d_3/50% D_2O (v/v), adjusted with 0.1 M DCl to pH 2.5. For the first 80 min, one-dimensional ^{1}H NMR spectra were obtained; subsequently, COSY spectra with a 22 min data collection time were recorded using 2048 complex data points, 4 transients, and 385 complex increments. Exchange rate constants were derived from least-squares fit of the cross-peak volume to the equation: $\ln(v) = -kt + C$, where v is the cross-peak volume normalized by the internal standard (nonexchangeable proton) at time t, k is the first-order exchange rate constant (min^{-1}), t is the elapsed time (min) after the peptide was dissolved, and C is the logarithm of the cross-peak volume at dead time.

Circular Dichroism. Circular dichroism spectra were recorded on a Jasco J-500 C spectropolarimeter (Jasco, Eaton, MD) equipped with a Jasco DP500N data processor. A Lauda (Model RMS) water bath (Brinkman Instruments, Rexdale, Ontario, Canada) was used to control the temperature of the cuvette. The temperature dependence of the molar ellipticity was measured at 220 nm by varying the temperature in the range of 5−65 °C. The peptides were dissolved in a 50% TFE/50% buffer solution (20 mM potassium phosphate and 50 mM KCl at pH 3) to a final concentration of 0.65 mg/mL as determined by amino acid analysis. Calculation of helical content was performed according to Chen et al. (1974):

$$f_H = \frac{[\Theta]_{220}}{[\Theta]_{220}^{\infty}} + \frac{ik}{N}$$

where f_H is the helix fraction, $[\Theta]_{220}$ the observed mean residue ellipticity at wavelength 220 nm, i the number of helical segments, k a wavelength-dependent constant (2.6 at 220 nm), N the total number of residues, and $[\Theta]_{220}^{\infty}$ the reference mean ellipticity for 100% helix (Yang et al., 1986). The CD experiments were repeated at various peptide concentrations down to the sensitivity limit of the spectrometer. The helicity values stayed constant, and no concentration dependence was observed, which also establishes the monomeric state.

3D Structure Calculations. The structures of the peptide DA-18 were calculated by using the Kollman all-atom force field within the environment of the SYBYL molecular modeling package V 6.1 (Tripos, Inc., St. Louis, MO) on a Silicon Graphics Indigo 2 R8000. The restraint categories used for NOE distances were strong (upper boundary 2.5 Å), medium (upper boundary 2.9 Å), weak (upper boundary 3.5 Å), and very weak (upper boundary 5.0 Å). A penalty constant of 50 kcal was used for 32 distance (NOE) restraints in the conformation calculations. In order to avoid hydrogen bonds at position D-Ala^9 (see NH exchange studies), we introduced additional distance restraints. A penalty constant of 200 kcal and a lower boundary of 3.0 Å at distances from the amide proton (residue D-Ala^9) respectively from the carboxyl oxygen to possible corresponding backbone hydrogen acceptors/donators force the observed conditions. Conformation space sampling was carried out using a distance-restrained simulated annealing protocol. The initial structure was minimized (Powell) in 3000 steps with included Coulomb interactions (Kollman dictionary charges). The annealing procedure used consists of 10 cycles of temperature ramping. The system was held after heating on a start temperature of 700 K for a plateau of 2 ps with a following five-step temperature cooling (to 200 K) phase of 10 ps. The 10 different low-temperature conformations that resulted were used after a 3000-step minimization as start conformations in the following molecular dynamics simulations at 300 K. After an equilibration phase of 5 ps with velocity scaling a constant temperature simulation at 300 K for 95 ps was carried out.

RESULTS

Design of the Model Peptides. In the present study a model peptide (LA-18) with a high intrinsic α-helical propensity according to Chou and Fasman (1978) and Eisenberg (1984) criteria was designed. The distribution of hydrophilic lysines and hydrophobic alanines and leucines is characteristic of an amphipathic helix and is displayed in Figure 1 in the helical wheel projection as well as in the helical cylinder model. In initial studies the replacement at positions 9 and 10 of LA-18 exhibited the largest effect on the peptide helicity and retention time and was selected for this study.

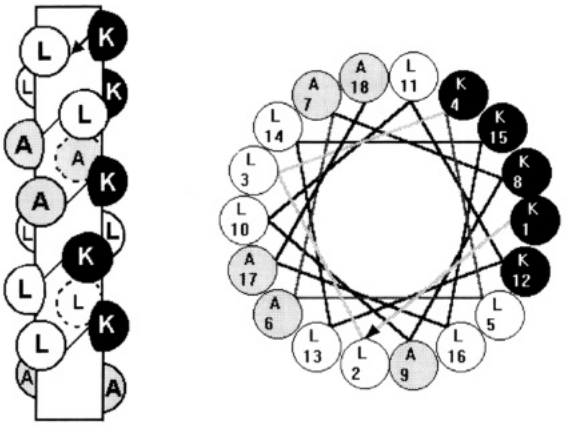

FIGURE 1: Amino acid sequences of the amphipathic peptide Ac-KLLKLAAKALLKLLKLAA-NH_2 represented in cylinder and helical wheel projections. The distribution of polar residues is indicated by black circles.

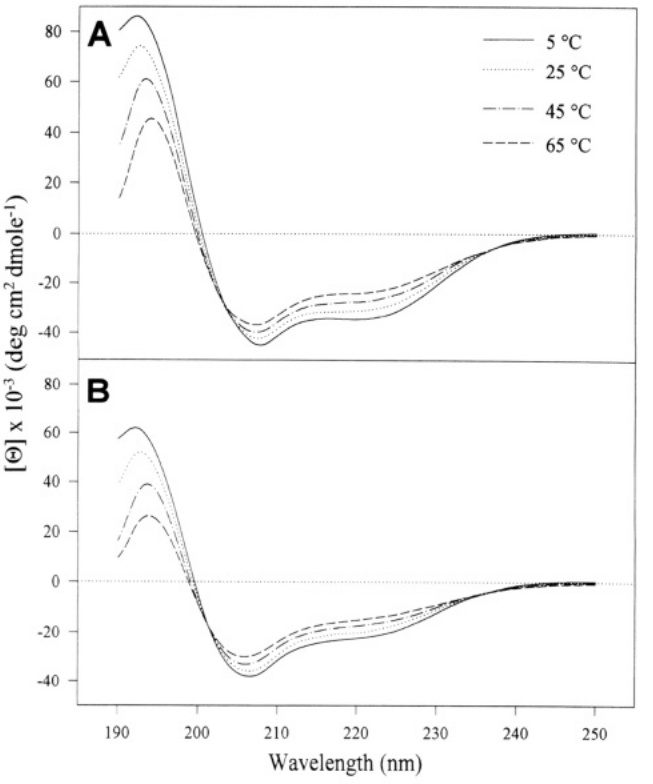

FIGURE 2: Circular dichroism spectra of LA-18 (A) and DA-18 (B) under varying temperatures in the presence of 50% α-helix-inducing solvent, trifluoroethanol, and at pH 3.0 (20 mM potassium phosphate and 50 mM KCl).

CD Experiments. CD spectra were obtained for the peptides LA-18 and DA-18 dissolved in a 50% aqueous solution of the helix-inducing solvent TFE (Figure 2). The spectra are characteristic for helical conformations and show two minima at 220 nm ($n\pi^*$ transitions) and at 206 nm ($\pi\pi^*$ transitions) as well as a maximum at 192 nm ($\pi\pi^*$ transitions). Using the equation for chain-length dependency of

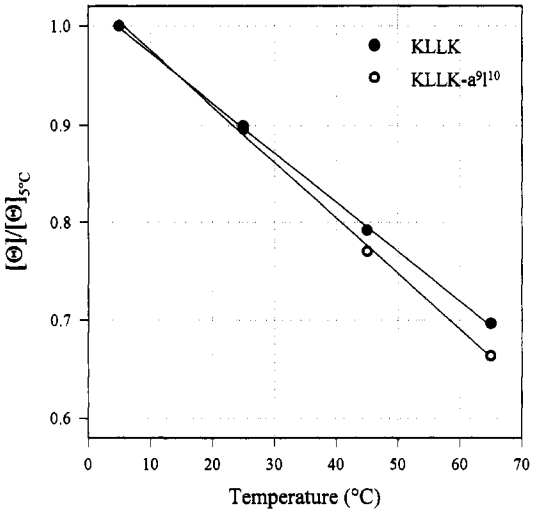

FIGURE 3: Thermal melting profiles of LA-18 and DA-18 in the presence of 50% trifluoroethanol and at pH 3.0 (20 mM potassium phosphate and 50 mM KCl). $\Theta_t/\Theta_{5\ °C}$ represents the ratio of the ellipticity at 220 nm at the indicated temperature to the ellipticity at 220 nm and 5 °C.

the expected molar ellipticity (Chen et al., 1974), the helicity for LA-18 was calculated to be 95% at 25 °C. The replacement of the two residues, Ala[9] and Leu[10], by their D-isomers led to a significant decrease of the helicity. The helicity was calculated to be 67% at 25 °C for DA-18 assuming one helix.

As discussed by Shortle (1989), the equilibrium between the native state and denatured state of polypeptides is a function of temperature, pH, and solution conditions. To investigate the stability differences arising from the D-amino acid replacements, the temperature dependence of the CD spectra (Zhu et al., 1993) was studied. As the temperature was increased, the mean molar ellipticity at 220 nm of both peptides decreased linearly, which is consistent with a loss of helicity. The isodichroic point at 202 nm is typical for a two-state transition from the α-helix to the random coil conformation (Padmanaban et al., 1990) and is indicative of thermal unfolding with increasing temperature. The observed ellipticities of −24 250 deg cm^2 dmol^{-1} for LA-18 and −14 900 deg cm^2 dmol^{-1} for DA-18 at 65 °C are 70% and 66% of the observed ellipticities at 5 °C. Surprisingly, the results are very similar for both peptides: the differences of about 30% in the ellipticities for 5 and 65 °C are smaller than expected and indicate that the design yielded quite stable amphipathic helices. Moreover, almost identical slopes in the thermal melting profiles (Figure 3) manifest only slightly different thermal stabilities for LA-18 as well as DA-18. Therefore, the destabilizing effect of two incorporated D-amino acids on the remaining helical content in DA-18 is marginal.

NMR Spectroscopy. Complete ^{1}H NMR assignments were made by using the standard sequential assignment procedure (Wüthrich et al., 1984) and the main-chain-directed approach (Englander & Wand, 1987) on the basis of double-quantum-filtered COSY (DQF-COSY), TOCSY, and NOESY spectra. Table 1 shows the chemical shifts of the proton resonances of LA-18 and DA-18 in 50% TFE/50% H_2O solvent (pH 2.5, 25 °C). Any overlap of sequential NN(i,i+1) cross peaks as well as of cross peaks in the fingerprint (NH−C_αH) region of the NOESY spectrum was resolved by varying the temperature in the range from 25 to 45 °C, facilitating the complete sequential assignment.

Table 1: Proton Chemical Shifts of LA-18 and DA-18 in 50% TFE and 50% H_2O, pH 2.5, at 25 °C

residue	NH	C_αH	C_βH	C_γH	C_δH	C_ϵH
(a) Proton Chemical Shifts of LA-18						
−$COCH_3$		2.15				
Lys[1]	8.23	4.03	1.85	1.6/1.48	1.76	3.01
Leu[2]	7.82	4.24	1.69	1.71	0.99/0.93	
Leu[3]	7.30	4.16	1.84	1.70	1.00/0.92	
Lys[4]	7.72	4.11	1.93	1.47	1.63	3.00
Leu[5]	7.80	4.19	1.88	1.71	0.97/0.93	
Ala[6]	8.24	4.15	1.54			
Ala[7]	8.11	4.12	1.55			
Lys[8]	7.80	4.05	2.05/1.99	1.52	1.74	3.00
Ala[9]	8.03	4.15	1.56			
Leu[10]	8.23	4.17	1.81/1.50	1.81	0.93	
Leu[11]	8.13	4.11	1.90/1.64	1.87	0.94	
Lys[12]	7.71	4.03	2.03	1.65	1.76	3.00
Leu[13]	7.92	4.16	1.91/1.83	1.84	0.95/0.91	
Leu[14]	8.56	4.10	1.93/1.56	1.92	0.89	
Lys[15]	8.04	4.10	2.05	1.55		3.00
Leu[16]	8.05	4.21	1.98/1.94	1.69	0.94	
Ala[17]	8.41	4.20	1.52			
Ala[18]	7.92	4.29	1.53			
NH_2	7.17					
NH_2	6.89					
(b) Proton Chemical Shifts of DA-18						
−$COCH_3$		2.15				
Lys[1]	8.21	4.01	1.86	1.48	1.77	3.02
Leu[2]	7.83	4.21	1.69		0.98/0.91	
Leu[3]	7.27	4.14	1.84	1.69	0.99/0.91	
Lys[4]	7.74	4.08	1.99/2.02	1.47	1.63	3.03
Leu[5]	7.85	4.18	1.89/1.94	1.80	0.94/0.88	
Ala[6]	8.46	4.11	1.58			
Ala[7]	8.08	4.25	1.59			
Lys[8]	7.74	4.31	1.99	1.48	1.76	3.03
D-Ala[9]	7.85	4.46	1.51			
D-Leu[10]	8.04	4.13	1.80	1.62	0.97/0.92	
Leu[11]	8.05	4.11	1.76	1.76	1.0/0.93	
Lys[12]	7.85	4.02	1.92	1.50	1.62	3.02
Leu[13]	7.33	4.24	1.75	1.72	0.99/0.91	
Leu[14]	7.77	4.10	1.85	1.77	0.92/0.87	
Lys[15]	7.96	4.10	1.97	1.57	1.75	3.02
Leu[16]	7.77	4.23	1.9/1.93	1.6	0.97/0.92	
Ala[17]	8.23	4.21	1.51			
Ala[18]	7.91	4.28	1.52			
NH_2	7.15					
NH_2	6.87					

Figure 4A shows the low-field region of the ^{1}H NMR 2D NOESY spectra of LA-18. The most interesting spin systems around the position of D-amino acid replacement were linked in a sequence-specific manner using NN(i,i+1) cross peaks. For LA-18 we found an almost continuous pathway of 16 unambiguous NN(i,i+1) connectivities along the backbone starting with residue Lys[1] and extending up to residue Ala[18]. Only the sequential cross peak between Lys[15] and Leu[16] was too close to the diagonal to be observed. In an ideal helix the sequential distances $d\alpha N(i,i+1)$ and $dNN(i,i+1)$ are 3.5 and 2.8 Å, respectively; thus the NN(i,i+1) cross peak should be more intense than the αN(i,i+1) cross peak in the absence of flexibility. The observed ratio of NN(i,i+1) and αN-(i,i+1) intensities in the center of the helix with about 4.3 is in close agreement with the ratio for an ideal α-helix (3.8). In comparison to NN(i,i+1) intensities of residues 3−17 (reference value = 100%), weaker sequential NN(i,i+1) cross peaks at residues Lys[1] (50%), Leu[2] (80%), and Ala[18] (60%) as well as the absence of the αN(1,2) cross peak indicate some flexibility at the N- and C-termini. The secondary structure was determined by interpretation of medium-range NOE connectivities. Of particular relevance to this work,

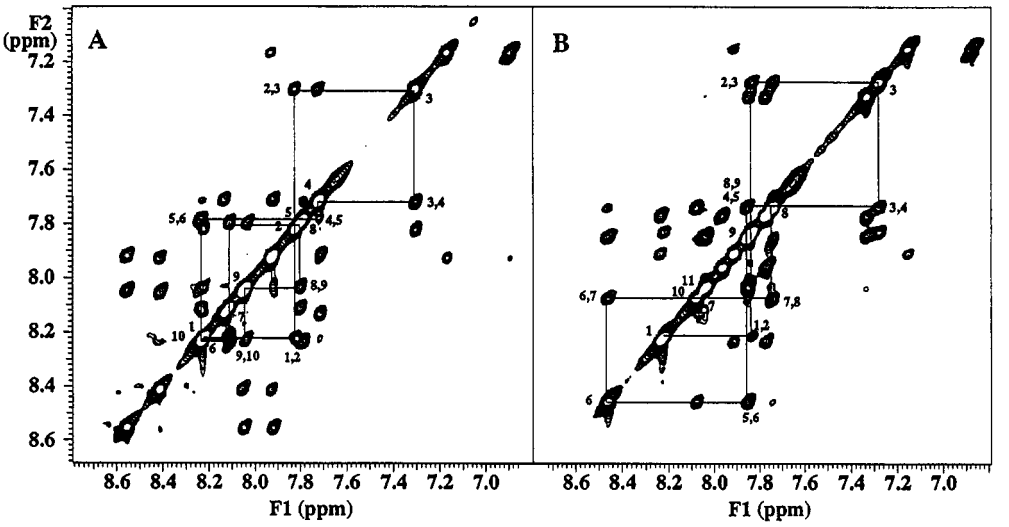

FIGURE 4: Amide region of the 500 MHz NOESY ^{1}H NMR spectra of LA-18 (A) and DA-18 (B) in 50% TFE/50% H_2O (v/v) at pH 2.5 and at 25 °C. Sequential NN(i,i+1) cross peaks from residue 1 to residue 10 are labeled.

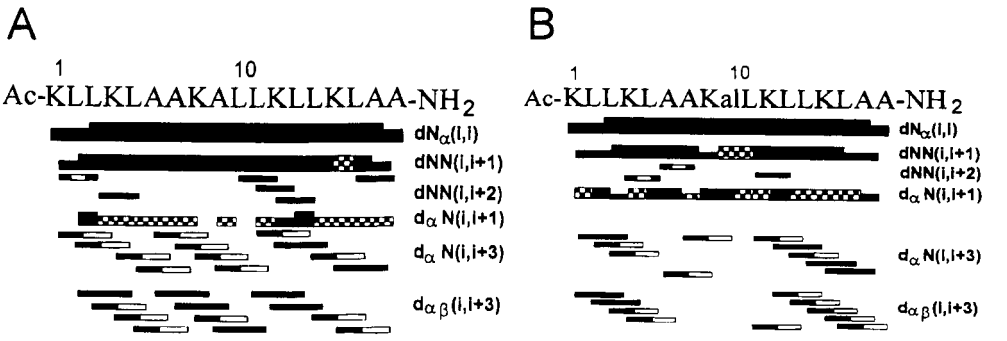

FIGURE 5: Summary of ^{1}H−^{1}H NOE connectivities for LA-18 (A) and DA-18 (B) in 50% TFE/50% H_2O (v/v) at pH 2.5 and at 25 °C. The intensity of NOE cross peaks is indicated by the thickness of the lines. Overlapping and therefore ambiguous cross peaks are indicated by checkered pattern.

the observation of medium-range αN(i,i+3) and αβ(i,i+3) NOE cross peaks (Wüthrich et al., 1984; Wright et al., 1988) is diagnostic for helical structure. Numerous αN(i,i+3) and αβ(i,i+3) NOEs along the entire sequence establish the presence of an ordered helix throughout the length of LA-18 (Figure 5A).

The results for DA-18 are very similar. As shown in the NN(i,i+1) region of the ^{1}H NMR 2D NOESY spectrum of DA-18 (Figure 4B) all the connectivities between Lys^1 and D-Ala^{10} as well as D-Leu^{11} and Ala^{18} were observable. Unfortunately, the similar amide proton shifts of D-Leu^{10} and L-Leu^{11} at all temperatures make the determination of the presence or absence of a sequential NN(10,11) NOE cross peak impossible. Furthermore, comparison of NOE intensities in temperature studies shows an overlap of a medium NN(4,5) and a weak NN(8,9) cross peak. Generally, the intensities of the sequential NN(i,i+1) cross peaks in the N-terminal part of DA-18 are somewhat more reduced (10−15%) than in the corresponding part in LA-18, suggesting a higher flexibility in the turn before the DD substitution. However, the most pronounced difference between LA-18 and DA-18 is located at the position of the D-amino acid replacement. The pattern of NOE connectivities is divided into two parts as shown in Figure 5. Neither medium-range αN(i,i+3) connectivities at positions 4, 7, 8, 9, and 10 nor αβ(i,i+3) cross peaks at positions 5, 6, 7, 8, and 9 were found. On the other hand, a number of medium-range αN(i,i+3) and αβ(i,i+3) NOEs were observed in two remaining segments (residues 1−5 and 11−18), indicating that the DD replacement has only a local influence on helical structure.

Proton Chemical Shift. It is well established that α-proton chemical shift deviations of amino acids from "random coil" reference values strongly correlate with the type of secondary structure (Clayden & Wilson, 1982; Dalgarno et al., 1983; Jimenez et al., 1987; Wishart et al., 1991). In particular, ^{1}H NMR shifts of Cα protons tend to experience an upfield shift (relative to random coil α-proton shifts) in α-helical structures and a downfield shift in β-strand or extended structures.

A plot of these α-proton secondary shift deviations *vs* the position along the sequence for LA-18 (Figure 6A) shows that the differences from random coil values were generally negative. Remarkably, all the resonances shifted upfield in a range from −0.33 to −0.05 ppm, which is consistent with an α-helical arrangement of the residues. According to a higher flexibility at the N- and C-terminus a weakly curved shape was obtained. In comparison, three significant downfield shifts were measured for DA-18 at positions Ala^7, Lys^8, and D-Ala^9. These residues are on the N-terminal side of the helix close to the position of D-amino acid replacement. A positive secondary shift of +0.13 ppm was observed for residue D-Ala^9 in DA-18 (versus the random coil shift for L-Ala). However, both curves are basically similar between residues 1−6 and 11−18, implying that these regions in DA-18 are not affected by D-amino acid replacement.

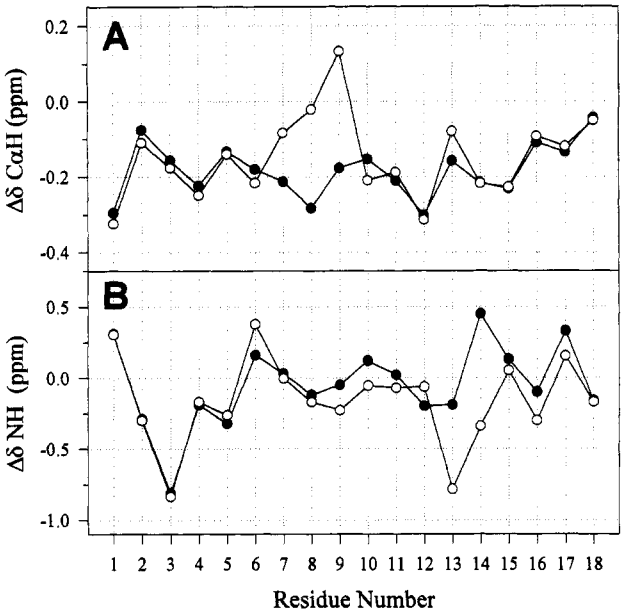

FIGURE 6: (A) Plot of ^{1}H NMR chemical shift differences between observed and random coil CαH shifts of LA-18 (●) and DA-18 (○) *vs.* the residue number. (B) Plot of chemical shift differences between observed and averaged NH shifts of LA-18 (●) and DA-18 (○) *vs* the residue number. The reference values for the random coil and averaged shifts (α-helix) are taken from Wishart et al. (1991,1995). All shifts were recorded in 50% TFE/50% H_2O (v/v) at pH 2.5 and at 25 °C.

The plot of differences between observed amide proton shifts and averaged helix shifts [reference values from Wishart et al. (1991)] for LA-18 *vs* the amino acid position is shown in Figure 6B. Most of the NH values are close to 0 ppm and therefore typical for a helical arrangement. According to the position in the hydrophobic face a weak periodicity of Δδ NH values was obtained with four maximum values on positions 6, 10, 14, and 17. The deviation for the first helix turn, especially the Δδ NH value of −0.81 ppm for Leu^3, is probably due to the lack of partners for hydrogen bonding and due to magnetic anisotropy between the acetyl group and NH for Leu^3. Similar deviations of Δδ NH values (−0.8 to −1.2 ppm) for the third residue of acetylated peptides were found by Blanco et al. (1992).

A comparison of Δδ NH values between LA-18 and DA-18 (Figure 6B) suggests that the replacement of two amino acids by their D-isomers has a very local influence on the electronic behavior. The shapes of both curves are very similar, and only two significant changes were obtained. These changes were found at Leu^{14} (−0.8 ppm) and at Leu^{13} (−0.6 ppm). In LA-18 both of these amide protons are hydrogen bonded with the corresponding carbonyl oxygen of Ala^9 and Leu^{10}. Thus, these large chemical shift changes also support a distortion of the secondary structure and/or an increased water/TFE accessibility at the position of the D-amino acid replacement.

Hydrogen Exchange. It has been demonstrated that at low pH values of 3−4 exchange rates of amide protons in peptides are at their minimum (Linderstrom-Lang, 1955; Wüthrich & Wagner, 1979). Under these conditions hydrogen exchange rates were obtained by directly monitoring the disappearance of the amide proton resonances as a function of time after being dissolved in TFE/D_2O at 25 °C and pH 2.5 (Figure 7). Overlap of amide proton resonances was solved by recording COSY spectra and following the exchange by the intensity of the αN(*i*,*i*) cross peaks. The results of the observed exchange rates of LA-18 and DA-18 are summarized in Table 2.

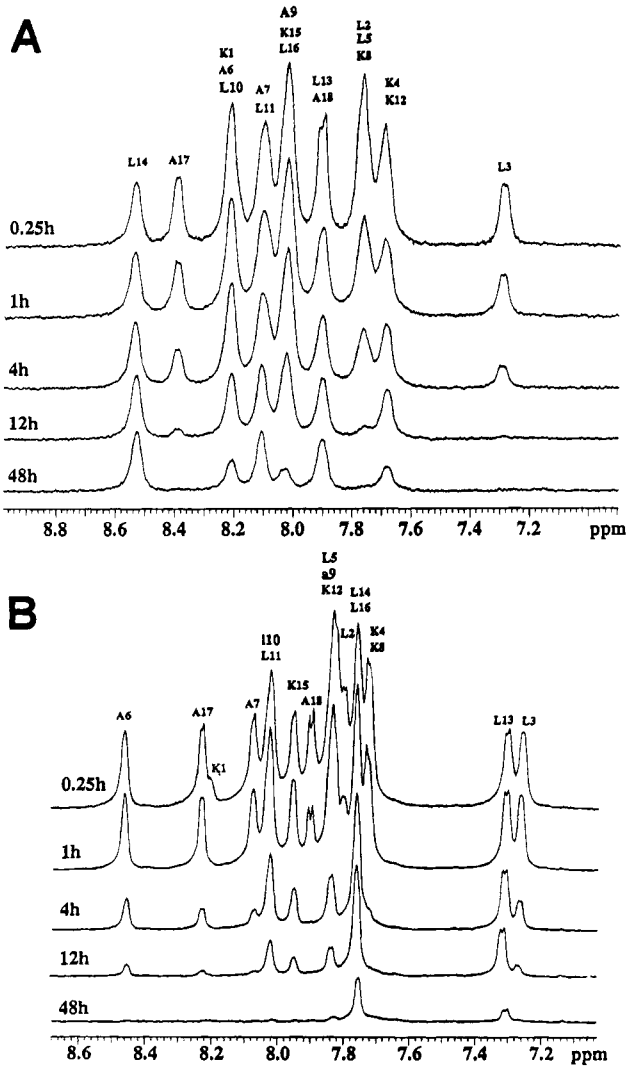

FIGURE 7: One-dimensional spectra of the amide proton resonances of LA-18 (A) and DA-18 (B) as a function of time after the peptides were dissolved in 50% TFE/50% D_2O (v/v) at pH 2.5 and at 25 °C.

Table 2: Hydrogen Exchange[a] for Backbone Amide Protons of LA-18 and DA-18

residue	LA-18	DA-18	residue	LA-18	DA-18
Lys^1	fast	fast	Leu^{11}	slow	slow
Leu^2	fast	fast	Lys^{12}	slow	medium
Leu^3	medium	medium	Leu^{13}	slow	slow
Lys^4	fast	fast	Leu^{14}	slow	slow
Leu^5	medium	medium	Lys^{15}	medium	medium
Ala^6	slow	medium	Leu^{16}	slow	slow
Ala^7	slow	medium	Ala^{17}	medium	medium
Lys^8	medium	medium	Ala^{18}	fast	fast
Ala^9/D-Ala^9	slow	fast	NH_2	fast	fast
Leu^{10}/D-Leu^{10}	slow	slow	NH_2	fast	fast

[a] In 50% TFE-d_3 and 50% D_2O, pH 2.5, at 25 °C. Fast, medium, and slow exchange is related to amide proton exchange rates $k_{NH} > 5 \times 10^{-3}$ min^{-1}, 1×10^{-3} min^{-1} < k_{NH} < 5×10^{-3} min^{-1}, and $k_{NH} < 1 \times 10^{-3}$ min^{-1}, respectively.

With the exception of Lys^8 and Lys^{15} in LA-18 we obtained lower exchange rates toward the middle of the sequence as expected for a stable helix. Protons at the N-terminus exchange faster than protons at the C-terminus

Table 3: Upper and Lower Boundary of Φ, Ψ Torsion Angles Appearing in the Common Low-Energy Conformation Pool Sampled from MD Runs

torsion angle		residue						
		Ala[6]	Ala[7]	Lys[8]	D-Ala[9]	D-Leu[10]	Leu[11]	Lys[12]
Φ	upper bound	−43	−51	+51	+137	+76	−34	−43
Φ	lower bound	−82	−105	−60	+43	−64	−82	−87
Ψ	upper bound	−26	+36	−38	+79	−30	−25	−29
Ψ	lower bound	−56	−61	−166	+38	−124	−63	−59

(Lys[1] <1 h, Leu[2] 1 h, Ala[17] 13 h, Ala[18] 6 h). This can be explained by the presence of hydrogen bonds for C-terminal amide protons, while amide protons in the first N-terminal helical turn are lacking hydrogen-bonding partners. Generally, the exchange rates for lysine are higher than for leucine or alanine. Considering previous results by Molday et al. (1972), who observed low exchange rates for lysines under acid-catalyzed conditions, a plausible explanation might be the increased solvent accessibility at the hydrophilic face in an amphipathic helix [see also Zhou et al. (1992)].

Similar exchange times at positions 1−5 and 13−18 suggest that the flexibility and/or the solvent accessibility of these helical regions is comparable in both peptides. It is interesting to note that the amide proton resonance of D-Ala[9] in DA-18 disappears within 5 h, while the amide proton of L-Ala[9] in LA-18 exchanges much slower. Similarly, the amide proton of Lys[12] in DA-18 exchanges faster than in LA-18. This can be explained by a good solvent accessibility at the peptide link between Lys[8] and D-Ala[9] and a resulting weaker hydrogen bond between the carbonyl group of Lys[8] and the corresponding amide proton of Lys[12]. The medium exchange rates of Ala[6] and Ala[7] and the large exchange rate for D-Ala[9] in DA-18 (all rates are small in LA-18) suggest that a structural change and a larger solvent accessibility are located in the region Ala[6] to D-Ala[9] of the peptide. The unexpected small exchange rate of D-Leu[10] might be due to a solvent shielding of the hydrophobic face of the more stable second helix.

3D Structure Calculations. All generated SA structures which fulfilled the experimental conditions (amide proton exchange and NOE-based restraints) served as starting conformations in MD simulations. All conformations within a range of 15 kcal/mol above the lowest potential energy observed in each MD run were sampled in a common pool. Analyzing the Φ, Ψ torsion angles of all pool conformations shows more or less α-helix typical values except for residues 8−10 (Table 3). Interestingly, on one hand the Φ−Ψ values of residue D-Ala[9] are in a Ramachandran plot (Figure 8B) located in an area typically for left-handed α-helix values. On the other hand, typical angles of a β-turn or further features were not detected in between Lys[8] and D-Leu[10]. The Φ and Ψ values of residue Lys[8] are clustered at an area of random coil angles (Figure 8). The calculated structures expose as two parts of right-handed α-helical conformation from residues 2 to 7 and 11 to 17 interrupted by a more or less flexible part. Superimposition of the helical part from residues 12 to 17 (Figure 9) demonstrates a distinct helix interruption between residues 8 and 10. The mutual orientation of the two helix parts varies from straight in line over

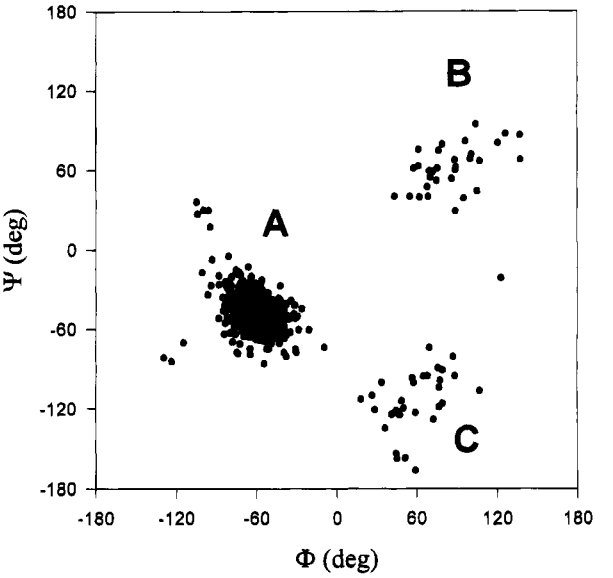

FIGURE 8: Φ−Ψ plane of 33 DA-18 structures obtained from 3D structure calculations. The plot shows all Φ and Ψ dihedral angles of the two helical regions 1−7 and 11−18 (A), D-Ala[9] (B), and D-Leu[10],Lys[8] (C).

weakly kinked to perpendicular arranged. Flexibility in the residue 8−10 area is observed, but rather to a certain degree (see also Φ and Ψ angles in Table 3). The kinked helices are arranged in a preferred space represented by three shaded ribbons in Figure 9.

DISCUSSION

The peptide LA-18 and its double D-amino acid analog DA-18 have been used to elucidate the influence of two adjacent D-amino acids on the conformation in amphipathic α-helices. The unsubstituted peptide LA-18 has a high helical propensity estimated by CD to be 95% in the presence of 50% TFE at 25 °C. DA-18 under identical conditions shows a considerably lower helical content of 67%. This suggests that the replacement of two adjacent L-amino acids by their D-isomers in the center of an 18-mer helix reduces the helical content by 28%. On the other hand, the comparison of the stability of LA-18 and DA-18 determined by thermal denaturation CD studies shows only a smaller effect. In 50% TFE the difference between the slopes of the melting profiles, which are related to the peptide stability, is less than 10% in a range of 5−65 °C.

While CD spectroscopy can only provide an average measure of the helical content of a peptide, two-dimensional NMR spectroscopy provides local structural information. In the case of LA-18, the NMR results correlate well with the CD studies. A continuous pathway of sequential NN(i,i+1) connectivities along the LA-18 backbone starting at Lys[1] to Ala[18], negative differences between observed and random coil chemical shifts for all Cα protons, and even distribution of medium-range αN(i,i+3) and αβ(i,i+3) NOEs over the entire sequence suggest a stable α-helix throughout the length of LA-18. In a similar way, the hydrogen exchange studies support these findings. Low exchange rates for the main part of LA-18 from residue 3 to residue 17 suggest the presence of intramolecular hydrogen bonds and good solvent shielding. Only the exchange rates at the N-terminus are large, which is expected for an α-helix due to the increased solvent accessibility and the lack of intramolecular hydrogen

FIGURE 9: Superimposition of the backbone (N, Cα, C) atoms of 33 DA-18 structures obtained from 3D structure calculations. The structures are best fitted to residues 11−16.

bond partners for the first three residues. The exchange rates at positions Lys[4], Lys[8], and Lys[15] imply an intact, bent-like amphipathic structure with increased solvent accessibility at the hydrophilic face. According to a maximum solvent shielding very low exchange rates were observed for amide protons at the corresponding hydrophobic face.

For DA-18 the NMR experiments indicate a somewhat higher helical content than estimated by CD spectroscopy. The continuous pathway of all sequential NN(i,i+1) and αN-(i,i+1) NOEs was present. Additionally, the more stringent criterion for an α-helix, medium-range αN(i,i+3) and αβ-(i,i+3) NOEs, is observed exclusively before as well as after the D-amino acid replacement. Applying the criteria for secondary structure prediction based on chemical shift data (Wishart et al., 1991, 1995), all CαH shifts were found to be characteristically for an α-helix, with D-Ala[9] being the only exception. This result agrees well with hydrogen exchange studies and the observation of a weak NN(8,9) cross peak of DA-18. In fact, the significantly accelerated exchange of the D-Ala[9] amide proton (<5 h) in comparison to the slow exchange of the L-Ala[9] amide proton in LA-18 (>48 h) indicates an increased solvent accessibility at the peptide link between Lys[8] and D-Ala[9].

Similar helix-breaking behavior has been observed in myoglobin, where a β-turn sequence (His[119]-Pro[120]-Gly[121]-Asp[122]) acts as a helix stop signal (Shin et al., 1993). Molecular dynamic calculations of β-turn model peptides suggested that the energetically favorable conformation for two adjacent D-amino acids (D-Ala-D-Ala) in short peptides is the type I′ β-turn (Yan et al., 1993). Also Yan and Erickson (1994) recently proposed that a pair of D-amino acids in the β-sheet protein betabellin 14D might favor type I′ β-turns. With regard to the identification of turns in peptides by NMR (Venkatachalan et al., 1968; Nemethy & Scheraga, 1980; Wüthrich et al., 1984; Dyson et al., 1988) neither characteristic strong NN(i+2,i+3) nor weak αN-(i+1,i+3) NOE connectivities were observed in this study. Compared to LA-18 the hydrogen exchange rate at position Lys[12] in DA-18 is notably increased, indicating the absence of a strong, turn-characteristic hydrogen bond between D-Ala[9] and Lys[12].

In summary, the NMR results obtained in 50% TFE suggest that (i) LA-18 adopts an amphipathic α-helix over the entire chain length with a small content of fraying at the N- and C-terminus, (ii) double D-amino acid replacements in the center of the sequence are interrupting the helix into two separate helices (residues 1−7 and 11−18), and (iii) the peptide bond between Lys[8] and D-Ala[9] shows a high degree of water accessibility and a high degree of flexibility. The CD results can also be interpreted on the assumption that the D-amino acid replacement will interrupt a continuous helix, and the observed ellipticity will then result from two, significantly shorter helices. After correction for the number of helical fragments the observed ellipticity of −20 200 deg cm^2 dmol^{-1} corresponds to 85% helicity. This result is in good agreement with the 83% helicity, expected for a peptide of 18 residues, in which two separate, stable helices of 7 and 8 residues are formed.

It is interesting to note that we found no reasonable correlation between hydrogen exchange rates and amide proton shift differences (see Figure 6B) under acid-catalyzed conditions. The upfield amide proton shift of Leu[13] in DA-18 and the opposite downfield shift of Leu[13] in LA-18 do not correlate with the exchange rates for the amide protons. We observed a very slow exchange for the amide proton at residue Leu[13] of greater than 48 h in both peptides. A similar discrepancy was obtained at residue Leu[3] where the strongest amide proton upfield shift does not correlate with the observed medium exchange rate. Recent NH exchange studies for helical model peptides (Rohl & Baldwin, 1994) are consistent with our findings and suggest that

acid-catalyzed exchange rates correlate with hydrogen bond formation by either the NH or the CO groups of a peptide unit. According to a split into two helices at position D-Ala[9] in the case of DA-18, the significant increase of the exchange rate of the amide proton at residue D-Ala[9] should be a result of two broken hydrogen bonds. However, if the amide proton shift differences are really related to the strength/length of intramolecular hydrogen bonds, this finding means that the stability against acid-catalyzed proton exchange is more complex and is affected by the hydrophobic environment in an amphipathic helix and by the formation of both hydrogen bonds at a residue.

Finally, considering the results of CD, NMR, and 3D structure calculations, the data suggest that two adjacent D-amino acids are interrupting the helical nature of the peptide LA-18, but reduce the number of residues being involved in helical conformation by only three residues. The results show that the incorporation of an adjacent pair of D-amino acids only causes a local change in structure and flexibility, which makes the double D-replacement interesting as a tool for specific helix-disturbing modifications to search for helical conformations in biologically active peptides.

ACKNOWLEDGMENT

The authors thank Annerose Klose for her assistance in peptide synthesis, Robert Luty for technical assistance in performing CD measurements, and Krishnakumar Rajarathnam, Key-Sun Kim, and Dave Wishart for critical and helpful discussions.

REFERENCES

Altmann, K.-H., Wojcik, J., Vasquez, M., & Scheraga, H. A. (1990) *Biopolymers 30*, 107−120.

Barlow, D. J., & Thornton, J. M. (1988) *J. Mol. Biol. 201*, 601−619.

Beck-Sickinger, A. G., Gaida, W., Schnorrenberg, G., Lang, R., & Jung, G. (1990) *Int. J. Pept. Protein Res. 36*, 522−530.

Blanco, F., Herranz, J., Gonzales, C., Jimenez, M., Rico, M., Santoro, C., & Nieto, J. (1992) *J. Am. Chem. Soc. 114*, 9676−9677.

Braunschweiler, L., & Ernst, R. R. (1983) *J. Magn. Reson. 53*, 521−528.

Chakrabartty, A., Schellman, J. A., & Baldwin, R. L. (1991) *Nature 351*, 586−588.

Chen, Y., Yang, J., & Chau, K. (1974) *Biochemistry 13*, 3350−3359.

Chou, P. Y., & Fasman, G. D. (1974) *Biochemistry 13*, 211−245.

Clayden, N. J., & Williams, R. J. P. (1982) *J. Magn. Reson. 49*, 383−396.

Dalgarno, D. C., Levine, B. A., & Williams, R. J. P. (1983) *Biosci. Rep. 3*, 443−452.

Davies, P. L., & Bax, A. (1985) *J. Am. Chem. Soc. 107*, 2820−2821.

Dyson, H. J., Rance, M., Houghten, R. A., Lerner, R. A., & Wright, P. E. (1988) *J. Mol. Biol. 201*, 161−200.

Eisenberg, D., Weiss, R. M., & Terwilliger, T. C. (1984) *Proc. Natl. Acad. Sci. U.S.A. 81*, 140−144.

Englander, S. W., & Wand, A. J. (1987) *Biochemistry 26*, 5953−5958.

Fairman, R., Anthony-Cahill, S. J., & DeGrado, W. F. (1992) *J. Am. Chem. Soc. 114*, 5458−5459.

Gurunath, R., & Balaram, P. (1994) *Biochem. Biophys. Res. Commun. 202*, 241−245.

Henklein, P., Beyermann, M., Bienert, M., & Knorr, R. (1991) *Peptides 1990* (Girald, E., & Andreu, D., Eds.) Escom Science Publishers B.V., Leiden.

Hernandez, J. F., Kornreich, W., Rivier, C., Miranda, A., Yamamoto, G., Andrews, J., Tache, Y., & Rivier, J. (1993) *J. Med. Chem. 36*, 2860−2867.

Jackson, M., & Mantsch, H. (1992) *Biochim. Biophys. Acta 1118*, 139−143.

Jeener, J., Meier, B. H., Bachmann, P., & Ernst, R. R. (1979) *J. Chem. Phys. 71*, 4546−4553.

Jimenez, M. A., Nieto, J. L., Herranz, J., Rico, M., & Santoro, J. (1987) *FEBS Lett. 221*, 320−324.

Kaiser, E. T., & Kezdy, F. J. (1983) *Proc. Natl. Acad. Sci. U.S.A. 80*, 1137−1143.

Krause, E., Beyermann, M., Dathe, M., Rothemund, S., & Bienert, M. (1995) *Anal. Chem. 67*, 252−258.

Lau, S. Y. M., Taneja, A. K., & Hodges, R. S. (1984) *J. Chromatogr. 317*, 129.

Linderstrom-Lang, K. (1955) *Chem. Soc., Spec. Publ. No. 2*, 1−20.

MacArthur, M. W., & Thornthon, J. M. (1991) *J. Mol. Biol. 218*, 397−412.

Moldey, R. S., Englander, S. W., & Kallen, R. G. (1972) *Biochemistry 11*, 150−158.

Nelson, J. W., & Kallenbach, N. R. (1986) *Proteins: Struct., Funct., Genet. 1*, 211−217.

Nemethy, G., & Scheraga, H. A. (1980) *Biochem. Biophys. Res. Commun. 95*, 320−327.

O'Neil, K., & DeGrado, W. L. (1990) *Science 250*, 646−651.

Padmanabhan, S., Margusee, S., Ridgeway, T., Laue, T. M., & Baldwin, R. L. (1990) *Nature 344*, 268−270.

Peeters, L. T., Macielag, M. J., Depoortere, I., Konteatis, Z. D., Florance, J. R., Lessor, R. A., & Galdes, A. (1992) *Peptides 13*, 1103−1107.

Piantini, U., Sorensen, O. W., & Ernst, R. R. (1982) *J. Am. Chem. Soc. 104*, 6800−6801.

Pounny, Y., & Shai, Y. (1992) *Biochemistry 31*, 9482−9490.

Rance, M., Sorensen, O. W., Bodenhausen, G., Wagner, G., Ernst, R. R., & Wüthrich, K. (1983) *Biochem. Biophys. Res. Commun. 117*, 479−485.

Rohl, C. A., & Baldwin, R. L. (1994) *Biochemistry 33*, 7760−7767.

Rothemund, S., Krause, E., Beyermann, M., Dathe, M., Engelhardt, H., & Bienert, M. (1995) *J. Chromatogr. 689*, 219−226.

Scholtz, J. M., & Baldwin, R. L. (1992) *Annu. Rev. Biophys. Biomol. Struct. 21*, 95−118.

Segrest, J. P., De Loof, H., Dohlman, J. G., Brouilette, C. G., & Anantharamaiah, G. M. (1990) *Proteins: Struct., Funct., Genet. 8*, 103−117.

Shin, H.-C., Merutka, G., Waltho, J. P., Wright, P. E., & Dyson, H. J. (1993) *Biochemistry 32*, 6348−6355.

Shoemaker, K. R., Kim, P. S., York, E. J., Stewart, J. M., & Baldwin, R. L. (1987) *Nature 326*, 563−567.

Shortle, D. (1989) *J. Biol. Chem. 264*, 5315−5318.

Sönnichsen, F. D., Van Eyk, J. E., Hodges, R., & Sykes, B. D. (1992) *Biochemistry 31*, 8790−8798.

Strehlow, K. G., Robertson, A. D., & Baldwin, R. L. (1991) *Biochemistry 30*, 5810−5814.

Venkatachalam, C. M. (1968) *Biopolymers 6*, 1425−1436.

Wishart, D. S., Sykes, B. D., & Richards, F. M. (1991) *J. Mol. Biol. 222*, 311−333.

Wishart, D. S., Bigam, C. G., Holm, A., Hodges, R. S., & Sykes, B. D. (1995) *J. Biomol. NMR 5*, 67−81.

Wright, P. E., Dyson, H. J., & Lerner, R. A. (1988) *Biochemistry 27*, 7167−7175.

Wüthrich, K. (1986) in *NMR of Proteins and Nucleic Acids*, Wiley, New York.

Wüthrich, K., & Wagner, G. (1979) *J. Mol. Biol. 130*, 1−18.

Wüthrich, K., Billeter, M., & Braun, W. (1984) *J. Mol. Biol. 180*, 715−740.

Yan, Y., & Erickson, B. W. (1994) *Protein Sci. 3*, 1069−1073.

Yan, Y., Tropsha, A., Hermans, J., & Erickson, B. W. (1993) *Proc. Natl. Acad. Sci. U.S.A. 90*, 7898−7902.

Yang, J. T., Wu, C. S. C., & Martinez, H. M. (1986) *Methods Enzymol. 130*, 208−256.

Zhou, N., Zhu, B., Sykes, B. D., & Hodges, R. S. (1992) *J. Am. Chem. Soc. 114*, 4320−4326.

Zhu, B., Zhou, N., Kay, C. M., & Hodges, R. S. (1993) *Protein Sci. 2*, 383−394.

BI950854+